

# Multi-Channel Inverse Scattering Problem on the Line: Thresholds and Bound States

M. Braun, S. A. Sofianos, H. Leeb\*

*Physics Department, University of South Africa, Pretoria 0003, South Africa*

(Dated: December 20, 2018)

## Abstract

We consider the multi-channel inverse scattering problem in one-dimension in the presence of thresholds and bound states for a potential of finite support. Utilizing the Levin representation, we derive the general Marchenko integral equation for N-coupled channels and show that, unlike to the case of the radial inverse scattering problem, the information on the bound state energies and asymptotic normalization constants can be inferred from the reflection coefficient matrix alone. Thus, given this matrix, the Marchenko inverse scattering procedure can provide us with a unique multi-channel potential. The relationship to supersymmetric partner potentials as well as possible applications are discussed. The integral equation has been implemented numerically and applied to several schematic examples showing the characteristic features of multi-channel systems. A possible application of the formalism to technological problems is briefly discussed.

PACS numbers: 03.65.Nk

---

\* On leave from Atominstitut der Österreichischen Universitäten, Technische Universität Wien, Wiedner Hauptstraße 8-10, A-1040 Wien, Austria

## I. INTRODUCTION

The first attempt to extend the single-channel inverse scattering problem (ISP) on the line [1, 2, 3, 4, 5] to a wider class of  $N \times N$  coupled-channel potentials was made by Wadati and Kamijo [6] about 25 years ago. They derived a Marchenko equation associated with the  $N \times N$  Schrödinger equation on the entire line ( $-\infty < x < \infty$ ). The problem has also been discussed in detail by Calogero and Degasperis [7]. In these investigations the presence of threshold energies was not included and, most importantly, practical aspects of the implementation of the solution of the ISP were not considered. Twenty years later, the coupled-channel problem was taken further with the inclusion of thresholds [8] and numerical solution of the corresponding Marchenko equation.

The lack of progress can be attributed to several reasons. Firstly, the solution of the ISP presupposes the knowledge of the full reflection coefficient (moduli and phases) at all incident momenta  $q$ . This requirement can not be easily fulfilled, especially due to the missing phase information in standard experiments, a difficulty which is similar to the well known and longstanding phase problem in diffraction analysis [9, 10, 11]. Secondly, a profile with an unlimited support leads to tough numerical questions because the highly oscillatory behavior of the reflection coefficient makes the numerical procedure cumbersome and unstable. A third difficulty in the presence of bound states is the determination of the bound state normalization constants for the various channels which are crucial for a unique reconstruction of the underlying coupled-channel potential.

Coupled-channel inverse scattering techniques in one dimension have been considered and numerically implemented for specular reflection of polarized neutrons from plane surfaces of magnetized samples [12]. These problems contain neither thresholds nor bound states and can be treated by the available Marchenko equations. The formulation of coupled-channel inverse scattering techniques taking simultaneously into account thresholds and bound states would be a valuable progress, specifically for the design of semiconductor quantum devices and for the synthesis of quantum heterostructures with specific spectral properties [13]. In this context the spectral design of systems with specific bound states embedded in the continuum would be of great interest for application.

In the present work we focus on the formulation of equations and numerical procedures for the solution of the coupled-channel inverse scattering problem on the line including

thresholds. We also take into account bound states lying energetically below the thresholds of all channels, but exclude those embedded in the continuum of any channel. Furthermore, we point out that the neglect of bound states in the input of the inversion procedure results in a supersymmetric partner potential with the same reflection properties, but completely different spatial shape. To test the formulated inverse scattering procedure and their numerical implementation, model examples are considered. In these models the reflection coefficient has been evaluated using known profiles and employed as input in the inverse scattering equations to recover the original scattering profile. The agreement between the reconstructed and the original profile is an important measure for the quality of the inverse scattering procedure and a criterion for the reliability of the numerical methods.

In Sect. II we present the formalism and give the essentials for the derivation of the generalized Marchenko equation. Technical details concerning the evaluation of the corresponding integrals and the treatment of bound states are outlined in the Appendix A. Furthermore, we sketch briefly the formalism of supersymmetric quantum mechanics for coupled-channel systems with thresholds and the construction of supersymmetric partner potentials. The feasibility of the developed formalism is demonstrated in Sect. III, where we reconstruct successfully coupled-channel potentials from simulated reflection and bound state data for various two-channel systems. Examples with and without thresholds and bound states are considered. In Sect. IV we summarize our conclusions and discuss potential applications of this inverse scattering technique.

## II. FORMALISM

### A. The direct problem

The multi-channel Schrödinger equation in one dimension has the form (in appropriate units)

$$\left(-\frac{d^2}{dx^2} + \mathbf{V}(x) + \mathcal{E}\right) \mathbf{\Psi} = k^2 \mathbf{\Psi}, \quad (1)$$

where  $\mathbf{V}(x)$  is assumed to be a real symmetric  $N \times N$  potential matrix of finite support with matrix elements  $V_{ij}(x)$ ,  $i, j = 1, \dots, N$ . Without loss of generality we assume for convenience that  $\mathbf{V}(x)$  vanishes on the entire negative  $x$ -axis. The solution  $\mathbf{\Psi}$  is a  $N \times N$  matrix whose columns are formed by the  $N$  linearly independent solution vectors of (1) at

an incident momentum  $k$  and  $\mathcal{E}$  is a diagonal matrix containing the threshold energies  $\epsilon_i$ ,  $i = 1, \dots, N$ . We assume that the threshold energies,  $\epsilon_i$  are arranged in increasing order with the lowest (in most cases the entrance channel) set to zero,  $\epsilon_1 = 0$ . The special case of no thresholds,  $\mathcal{E} = 0$ , has already been considered by Wadati and Kamijo [6] in 1974. Here, we focus on the general case and allow the occurrence of non-vanishing thresholds,  $\epsilon_j > 0$  for  $j = 2, 3, \dots, N$ .

The free solutions are given by  $\exp(\pm i\mathcal{K}x)$ , where now  $\mathcal{K}$  is given by

$$\mathcal{K}^2 = k^2 \mathbf{1} - \mathcal{E},$$

$\mathbf{1}$  being the  $N$ -dimensional unit matrix. The matrix  $\mathcal{K}$  is diagonal and is defined on the physical sheet of the Riemann surface for the momentum variable  $k$ . This sheet has an  $(N - 1)$ -fold branch cut on the real axis on the upper rim of which  $k_1 = k$ , and the other diagonal elements of  $\mathcal{K}$  are defined as follows

$$k_j = \begin{cases} +\sqrt{k^2 - \epsilon_j} & \text{for } k \geq \sqrt{\epsilon_j} \\ +i\sqrt{\epsilon_j - k^2} & \text{for } |k| < \sqrt{\epsilon_j} \\ -\sqrt{k^2 - \epsilon_j} & \text{for } k \leq -\sqrt{\epsilon_j} \end{cases} \quad (2)$$

for  $j = 2, \dots, N$ .

Similarly to the one-channel case we introduce sets of linearly independent matrix Jost solutions  $\mathcal{F}_\pm(k, x)$ ,  $\tilde{\mathcal{F}}_\pm(k, x)$  defined by the boundary conditions

$$\lim_{x \rightarrow \pm\infty} \exp(\mp i\mathcal{K}x) \mathcal{F}_\pm(k, x) = \mathbf{1} \quad (3)$$

$$\lim_{x \rightarrow \pm\infty} \exp(\pm i\mathcal{K}x) \tilde{\mathcal{F}}_\pm(k, x) = \mathbf{1}. \quad (4)$$

The boundary condition  $\tilde{\mathcal{F}}_-(k, x)$ , for example, implies that each solution vector has at  $x \rightarrow -\infty$  only in one channel an incoming wave from the left ( $e^{ik_j x}$ ) and none in all other channels. It is therefore obvious that  $\tilde{\mathcal{F}}_-(k, x)$  will provide the incoming component of the physical solution  $\Psi_L(k, x)$  for incidence from the left. Because the Jost solutions form a complete set we can write the physical solution of (1) for left and right incidence in terms

of  $\mathcal{F}_\pm(k, x)$  and  $\tilde{\mathcal{F}}_\pm(k, x)$ ,

$$\begin{aligned}\Psi_L(k, x) &= \mathcal{F}_+(k, x)\mathcal{T}_L(k) \\ &= \tilde{\mathcal{F}}_-(k, x) + \mathcal{F}_-(k, x)\mathcal{R}_L(k),\end{aligned}\tag{5}$$

$$\begin{aligned}\Psi_R(k, x) &= \mathcal{F}_-(k, x)\mathcal{T}_R(k) \\ &= \tilde{\mathcal{F}}_+(k, x) + \mathcal{F}_+(k, x)\mathcal{R}_R(k).\end{aligned}\tag{6}$$

Here,  $\mathcal{R}_{L,R}(k)$  and  $\mathcal{T}_{L,R}(k)$  are the reflection and transmission coefficient matrices for left (L) and right (R) incidence of the beam, respectively.

In the absence of thresholds the members of each pair of solutions are related by replacing  $k$  by  $-k$ , i.e.  $\tilde{\mathcal{F}}_\pm(k, x) = \mathcal{F}_\pm(-k, x)$  (cf. [6]). In the presence of thresholds, however, this relation does not hold anymore for  $k^2 < \epsilon_N$  because of the  $N$ -fold connectivity of the  $k$ -plane [8]. Considering the symmetry of the transformation (2) and of the Schrödinger equation (1) it is obvious that the identities

$$\mathcal{F}_\pm(-k, x) = \mathcal{F}_\pm^*(k, x) \quad \text{and} \quad \tilde{\mathcal{F}}_\pm(-k, x) = \tilde{\mathcal{F}}_\pm^*(k, x)\tag{7}$$

are also satisfied in the presence of thresholds. A direct consequence of Eq. (7) is the symmetry property of the reflection and transmission matrices for real  $k$ ,

$$\mathcal{R}_{R,L}(-k) = \mathcal{R}_{R,L}^*(k) \quad \text{and} \quad \mathcal{T}_{R,L}(-k) = \mathcal{T}_{R,L}^*(k).\tag{8}$$

Introducing the matrix generalized Wronskian relation,

$$\begin{aligned}W[\Psi(k, x), \Phi(k, x)] &\equiv \Psi^T(k, x) \left( \frac{d}{dx} \Phi(k, x) \right) \\ &\quad - \left( \frac{d}{dx} \Psi^T(k, x) \right) \Phi(k, x),\end{aligned}\tag{9}$$

where  $\Psi$  and  $\Phi$  are solutions of the coupled-channel Schrödinger equation (1) and  $T$  denotes transposition, one obtains

$$\frac{d}{dx} W[\Psi(k, x), \Phi(k, x)] = 0.\tag{10}$$

This means that the Wronskian of two solutions of Eq. (1) is constant on the entire  $x$ -axis. Specifically, it vanishes for two linearly dependent solutions. Evaluating the Wronskian  $W[\Psi_L, \Psi_L] = 0$  in the limit  $x \rightarrow -\infty$  and using the relation of  $\Psi_L(k, x)$  given in Eq. (5), yields

$$\mathcal{R}_L^T \mathcal{K} = \mathcal{K} \mathcal{R}_L.\tag{11}$$

This relation clearly indicates the effect of the thresholds on the symmetry of the reflection matrix.

## B. Inverse Scattering Equation

The determination of the potential matrix,  $\mathbf{V}(x)$ , from the knowledge of the reflection matrix,  $\mathbf{R}_L(k)$  ( $\mathbf{R}_R(k)$ ), is known as inverse scattering problem and its solution can be obtained via integral equations, often referred as Marchenko equations, for several quantum systems. Recently, an integral equation for one-dimensional coupled-channel systems with thresholds has been presented [8]. The derivation did not include the presence of bound states which are essential features of realistic quantum systems. Here, we focus on the ISP of coupled-channel systems in one dimension including thresholds and bound states. In the following the essential aspects of the derivation are outlined.

The integral equation for the solution of the ISP associated with Eq. (1) is most easily obtained via the Levin representation [3, 5] of  $\mathcal{F}_\pm(k, x)$ ,

$$\mathcal{F}_+(k, x) = e^{+i\mathcal{K}x} + \int_x^{+\infty} dz \mathbf{B}_+(x, z) e^{+i\mathcal{K}z} \quad (12)$$

$$\mathcal{F}_-(k, x) = e^{-i\mathcal{K}x} + \int_{-\infty}^x dz \mathbf{B}_-(x, z) e^{-i\mathcal{K}z}. \quad (13)$$

Inserting these expressions into Eq. (1) leads after some algebraic manipulations to differential equations for the transformation kernels  $\mathbf{B}_\pm(x, y)$ ,

$$\left( \frac{\partial^2}{\partial x^2} - \frac{\partial^2}{\partial y^2} \right) \mathbf{B}_\pm(x, y) = \mathbf{V}(x) \mathbf{B}_\pm(x, y) + [\mathcal{E}, \mathbf{B}_\pm(x, y)], \quad (14)$$

where we have introduced the commutator  $[\mathcal{A}, \mathcal{B}] = \mathcal{A}\mathcal{B} - \mathcal{B}\mathcal{A}$ . The transformation kernels are related to the potential via

$$\mathbf{V}(x) = -2 \frac{d}{dx} \mathbf{B}_+(x, x^+), \quad \mathbf{V}(x) = 2 \frac{d}{dx} \mathbf{B}_-(x, x^-) \quad (15)$$

and satisfy the boundary conditions

$$\lim_{x, y \rightarrow \pm\infty} \mathbf{B}_\pm(x, y) = 0. \quad (16)$$

Thus for  $x = y$ ,

$$\mathbf{B}_-(x, x) = \frac{1}{2} \int_{-\infty}^x dz \mathbf{V}(z). \quad (17)$$

The above partial differential equations together with the boundary conditions (16) and (17) constitute a Goursat problem [5] of a generalized nature.

Because of the restriction placed on the potentials, the existence of solutions for the partial differential equation (14) under the above boundary conditions, can be easily shown as follows: A change of variables to  $u = \frac{1}{2}(x - y)$  and  $v = \frac{1}{2}(x + y)$  transforms (14) into

$$\frac{\partial^2 \mathbf{B}_-}{\partial u \partial v} = \mathbf{V}(u + v) \mathbf{B}_- + [\mathcal{E}, \mathbf{B}_-] ; \quad (18)$$

A formal iterative solution of this partial differential equation involves repeated integrations over the potential. Since we imposed the condition of finite support on  $\mathbf{V}$  this series will converge, due to the triangular nature of domains over which the integrations take place.

The corresponding Marchenko integral equation is obtained by multiplying Eq. (5) from the right with

$$\frac{1}{2\pi} \exp(-i\mathcal{K}y) \frac{d\mathcal{K}}{dk} = \frac{1}{2\pi} \exp(-i\mathcal{K}y) \mathcal{K}^{-1} k , \quad (19)$$

substituting the Levin representations for  $\mathcal{F}_-(k, x)$  and  $\tilde{\mathcal{F}}_-(k, x)$  on the right hand side and integrating over  $k$ . Restricting ourselves to systems which have only bound states at negative energies ( $k^2 = q_\alpha^2 < 0$ ,  $\alpha = 1, \dots, N_b$ ) and assuming that no bound states are embedded in the continuum, we can evaluate the relevant integrals (see Appendix A). The result can be cast into the form

$$\mathbf{B}_-(x, y) + \boldsymbol{\rho}_-(x, y) + \int_{-\infty}^x dz \mathbf{B}_-(x, z) \boldsymbol{\rho}_-(z, y) = 0 . \quad (20)$$

where  $x > y$ . The input kernel of the above integral equation is given by

$$\boldsymbol{\rho}_-(x, y) = \tilde{\boldsymbol{\rho}}_-(x, y) + \tilde{\boldsymbol{\rho}}_-^{(b)}(x, y) \quad (21)$$

with

$$\tilde{\boldsymbol{\rho}}_-(x, y) = \frac{1}{\sqrt{2\pi}} \int_{-\infty}^{+\infty} dk e^{-i\mathcal{K}x} \mathcal{R}_L(k) e^{-i\mathcal{K}y} , \quad (22)$$

$$\tilde{\boldsymbol{\rho}}_-^{(b)}(x, y) = -i \sum_{\alpha=1}^M e^{-i\mathcal{Q}_\alpha x} \mathcal{M}_\alpha e^{-i\mathcal{Q}_\alpha y} \mathcal{Q}_\alpha^{-1} q_\alpha , \quad (23)$$

and  $\mathcal{Q}_\alpha = \mathcal{K}(q_\alpha)$ .

### C. Determination of the Input Kernel

An important step for the application of the inverse scattering procedure is the determination of the input kernel  $\rho_{-}(x, y)$  from the scattering data. Using the relation  $\mathcal{R}_L(k) = \mathcal{R}_L^*(-k)$  one can immediately evaluate the contribution of the continuum spectrum,  $\tilde{\rho}_{-}(x, y)$ . The bound state contribution,  $\tilde{\rho}_{-}^{(b)}(x, y)$  requires the knowledge of the bound state energies  $q_{\alpha}^2$  and the corresponding asymptotic normalization matrices  $\mathcal{M}_{\alpha}$ . If these quantities are obtained from simulated data, assuming a given potential  $\mathcal{V}(x)$ , then the inversion procedure should yield the original potential. In spectral design, however, these quantities are not available except when one is interested to have a bound state at a specific energy. In such a case arbitrary values of  $\mathcal{M}_{\alpha}$ , may result in a rather extended profile which is of limited interest because it can not easily be materialized.

To ensure that the inverse scattering procedure provides us with a potential  $\mathcal{V}(x)$  which vanishes for  $x < 0$  we must look for the required characteristics of  $\rho_{-}(x, y)$ . From the Levin representation of  $\mathcal{F}_{-}$ , Eq. (13) it follows that  $\mathcal{B}_{-}(x, y)$  vanishes identically for  $x < 0$ . Because of Eq. (20), the input kernel  $\rho_{-}(x, y)$  must also vanish for  $y < x < 0$  and Eq. (21) reduces for  $x < 0$  to the identity

$$\begin{aligned} \tilde{\rho}_{-}(x, y) &= -\tilde{\rho}_{-}^{(b)}(x, y) \\ &= i \sum_{\alpha=1}^{\infty} \exp(-i\mathcal{Q}_{\alpha}x) \mathcal{M}_{\alpha} \exp(-i\mathcal{Q}_{\alpha}y) \mathcal{Q}_{\alpha}^{-1} q_{\alpha} \end{aligned} \quad (24)$$

where  $y < x < 0$ . This relation is formally equivalent to the one-channel case [14] and expresses the fact that the potential  $\mathcal{V}(x)$  can be forced to vanish for  $x < 0$  if there is a series of bound states with binding energies  $q_{\alpha}^2$  and normalizations  $\mathcal{M}_{\alpha}$  which compensate  $\tilde{\rho}_{-}(x, y)$ .

Because of the peculiar spatial form of the contribution, it is obvious that those bound states which are energetically closest to threshold determine the behavior of the potential at large negative  $x$ -values. Thus for practical applications, we firstly assume to have a finite number,  $N_b$ , of bound states, and restrict ourselves to those energetically closest to threshold. With a fixed number  $N_b$  of bound states, it is then possible to deduce the bound state parameters solely from the knowledge of  $\mathcal{R}_L$  via the nonlinear Eq. (25). We may solve this equation in two steps. Since the diagonal elements of  $\mathcal{B}_{-}(x, y)$  only depend on  $x + y$ , a one dimensional fit to the sum of exponentials will produce the  $q_{\alpha}$ -values and the diagonal



elements of  $\mathcal{M}_\alpha$ . The knowledge of the  $q_\alpha$  values is then sufficient to obtain the remaining non diagonal elements of the  $\mathcal{M}_\alpha$ . Therefore, the kernel  $\rho_-(x, y)$  can be recovered and the determination of the potential can be achieved via the Marchenko equation. It should be noted that in the presence of thresholds, the input kernel  $\rho_-(x, y)$  depends on the variables  $x$  and  $y$  separately, while in the case of no thresholds it depends on the sum  $x+y$ . Furthermore, the input kernel has the symmetry property  $\rho_-(x, y) = \rho_-^T(y, x)$  because of the symmetry, Eq. (11), which implies  $\mathcal{R}_L \mathcal{K}^{-1} = \mathcal{K}^{-1} \mathcal{R}_L^T$ .

#### D. Supersymmetric Partners

The omission of the contribution of the bound state spectrum in  $\rho_-(x, y)$  leads via the inverse scattering procedure to a potential which generates the same reflection coefficient but does not sustain any bound state. This feature is characterizing phase-equivalent partner potentials which can be obtained easily via techniques of supersymmetric (SUSY) quantum mechanics [15, 16, 17]. The corresponding so-called SUSY transformations are based on the factorization method [18] which has been formulated to coupled-channel systems including thresholds [19, 20, 22]. A compact outline of the extension to coupled-channel systems is sketched in the following.

In the factorization method the Hamiltonian of the coupled Schrödinger equation (1) is written in the form

$$-\frac{d^2}{dx^2} + \mathcal{V}_0(x) = \hat{A}_0^+ \hat{A}_0^- - \mathcal{E} + \bar{q}^2, \quad (25)$$

where the factorization energy,  $\bar{q}^2$ , is smaller or equal to the energy  $q_1^2$  of the lowest bound state. The index 0 of  $\mathcal{V}(x)$  indicates that it is the original potential before any transformation. The factorization operators  $\hat{A}_0^\pm$  are given in terms of the superpotential  $\mathcal{W}_0(x)$ ,

$$\hat{A}_0^\pm = \pm \frac{d}{dx} + \mathcal{W}_0(x), \quad (26)$$

which satisfies the nonlinear differential equation

$$\frac{d}{dx} \mathcal{W}_0 + \mathcal{W}_0^2 = \mathcal{V}_0 + \mathcal{E} - \bar{q}^2. \quad (27)$$

It is straightforward to show that for any solution  $\Psi_0(k, x)$  of the original Schrödinger equation (1), the transformation  $\hat{A}_0^- \Psi_0(k, x)$  leads to a solution at the same energy  $k^2$  of the

coupled Schrödinger equation with the potential

$$\mathbf{V}_1 = \mathbf{V}_0 - 2\frac{d}{dx}\mathbf{W}_0. \quad (28)$$

If we choose the factorization energy  $\bar{q}^2 = q_1^2$ , one is able to eliminate the ground state from the spectrum of the original Hamiltonian (cf. [19, 20, 22]). The reflection matrix  $\mathcal{R}_1(k)$  associated with the transformed potential has changed, however,

$$\mathcal{R}_1(k) = (\mathbf{W}_0^- + i\mathcal{K})\mathcal{R}_0(k)(\mathbf{W}_0^- - i\mathcal{K})^{-1}. \quad (29)$$

Here,  $\mathbf{W}_0^\pm$  are the boundary values of  $\mathbf{W}_0$  at  $x \rightarrow \pm$ , respectively.

To restore the same reflection matrix  $\mathcal{R}(k)$  a second SUSY transformation at the same energy  $\bar{q}^2$  must be performed [19, 20] using the boundary values  $\mathbf{W}_0^- = -\mathbf{W}_1^- = -i\mathcal{Q}_1\mathcal{S}$ . Here  $\mathcal{S}$  is a diagonal matrix containing  $-1$  in the first  $M$  rows and  $+1$  in the remaining  $N - M$ , where  $M \leq N$  is the degeneracy of the ground state of the original system.

### III. EXAMPLES

As a demonstration of the coupled-channel inverse scattering equations, derived above, we consider several schematic examples which exhibit the specific features of coupled-channel systems. For the numerical implementation of the integral equation (20) we follow similar techniques as outlined in the appendix of Ref. [8].

First we consider the case of a two-channel system without a threshold and a bound state. We choose the potential  $\mathbf{V}(x)$  to have different  $x$ -dependence in the various matrix elements. We take a Gaussian shape for  $V_{11}(x)$  with the parameters  $V_0 = 0.1$ ,  $b = 4$ ,  $c = 1.8$  and a two layer repulsive profile ( $N = 2$ ) for  $V_{22}(x)$  with the parameters  $a = 0.01$ ,  $x_0 = 0.5$ ,  $V_1 = 0.08$ ,  $x_1 = 2.7$ ,  $V_2 = 0.05$ ,  $x_2 = 4.0$ . The off-diagonal elements  $V_{12}(x) = V_{21}(x)$  are given by an  $n_s = 3$  sea-saw potential with the parameters  $V_0 = 0.075$ ,  $x_\ell = 1.2$ ,  $x_s = 0.75$ ,  $s_1 = +1$ , and  $s_2 = s_3 = -1$ . A definition of the shapes and the parameters is given in Appendix B. With this potential we solved Eq. (1) and evaluated  $\mathcal{R}_L(k)$  up to  $k_{max} = 12$ . Using this  $\mathcal{R}_L(k)$ -values we reconstructed the potential  $\mathbf{V}(x)$  via the procedure given in Eqs. (20) to (25). The reconstructed potential matrix elements are displayed in Fig. 1 together with the original ones. It is seen that the reproduction of the original potentials is excellent.

Next we consider the case where thresholds are present. Again we use an input potential  $\mathbf{V}(x)$  which is chosen differently to the previous case in order to demonstrate the ability of

the algorithm to deal with rather different situations. The potential chosen is a Gaussian with parameters  $V_0 = 0.15$ ,  $b = 9$ ,  $c = 1.8$  for  $V_{11}(x)$ ; a one layer repulsive profile ( $N = 1$ ) with  $a = 0.05$ ,  $x_0 = 1.0$ ,  $V_1 = 0.20$ ,  $x_1 = 2.8$  for  $V_{22}(x)$ ; and Gaussian potentials with  $V_0 = 0.12$ ,  $b = 9$ ,  $c = 2.2$  for  $V_{12}(x) = V_{21}(x)$ . A threshold energy of  $\epsilon = 0.025$  is assumed in the second channel. The reconstruction from evaluated  $\mathcal{R}_L(k)$  data up to  $k_{max} = 12$  are shown in Fig. 2 and are once again in almost perfect agreement with the original. It is interesting to note here that although all elements of  $\mathcal{V}(x)$  are repulsive, the coupling of channels may lead to bound states. In the present example an increase of the strength of the coupling potential e.g. from  $V_0 = 0.12$  to  $V_0 = 0.5$  results in a bound state at  $E_b = -0.00053$ . This is in agreement with the observations made in Ref. [21].

An example of a two-channel system with a bound state, but without threshold is shown in Fig. 3. The potential is chosen to be of Gaussian form with  $V_0 = 0.15$ ,  $b = 1.5$ ,  $c = 2.2$  for  $V_{11}$ ; a one-layer profile with  $a = 0.1$ ,  $x_0 = 1.0$ ,  $V_1 = -0.1$  and  $x_2 = 3.3$ , for  $V_{22}$ . The off-diagonal profiles  $V_{12}(x) = V_{21}(x)$  are given by a sea-saw potential with  $V_0 = 0.1$ ,  $x_\ell = 1.5$ ,  $x_s = 0.70$ , and  $n_s = 2$ , with  $s_1 = s_2 = +1$ . The system sustains a bound state at  $E_b = -0.01558$  with  $M_{11} = -0.0065$ ,  $M_{12} = 0.0216$ ,  $M_{21} = 0.0216$ , and  $M_{22} = -0.0711$ . As expected, the off-diagonal asymptotic normalization constants are, in this case, the same. As one can see from Fig. 3, the reproduction of the potential is, for all practical purposes, perfect.

It is interesting to consider next the simultaneous existence of thresholds and bound states. For this we consider the previous example with a threshold  $\epsilon = 0.01$ ; the rest of the input data remaining the same. The presence of the threshold generates a bound state at  $E_b = -0.0068$  with  $M_{11} = -0.0104$ ,  $M_{12} = 0.0400$ ,  $M_{21} = 0.0257$ , and  $M_{22} = -0.1031$ . The reproduction of the potential is, once more, excellent.

As a final example, we consider the SUSY transformations. Setting the asymptotic normalization constants equal to zero results, as expected, in supersymmetric partner profiles displayed in Fig. 4 which do not sustain a bound state and look considerably different from the original ones.

It should be noted here that an insertion of a bound state at an arbitrary energy results in different values for the asymptotic normalization constants. When these constants are evaluated via (23), then the inversion procedure provides us always with the original interaction.

## IV. CONCLUSIONS

We have studied the inverse scattering problem on the line including thresholds and derived the corresponding integral equation of Marchenko type. Specific care was taken for the integrations on the physical sheet of the Riemann surface of the momentum variable  $k$  because of the  $(N - 1)$ -fold branch cut as discussed in Sect. IIA. We found that these branch cuts do not generate additional problems as long as we deal with systems sustaining only true bound states. The integration contour is well defined and the integrand satisfies all conditions required for the application of Cauchy's integral formula. In this way the resulting Marchenko equation can be applied when threshold and bound states are simultaneously present in the system.

Much emphasis was given to the application of the method which implies the numerical implementation as well as the generation of the input kernel  $\rho_-(x, y)$  from scattering data. Following the techniques outlined in Ref. [8] we achieved almost perfect numerical reconstructions as it can be seen from the examples given in Sect. III.

Furthermore, we considered the bound state contribution to  $\rho_-(x, y)$  which depends on the bound state energies and the so-called asymptotic normalization constants, where the latter are usually not accessible to experiment. We pointed out that the neglect of the bound state contribution results in a supersymmetric partner potential and leads to completely different profiles which, nevertheless, generate the same reflection coefficient matrix. Thus, the absence of bound state data may lead to wrong conclusions concerning the profiles.

We proposed a method for the determination of bound state data with regard to the design of quantum devices with pre-designed reflection properties. Thus, a profile of finite range can be extracted which might be utilized by nanotechnology. Although we can not force the profile to be limited to  $x > 0$ , the procedure allows to create non-vanishing profiles with a rather sharp edge at  $x = 0$ .

A severe problem for applications is the necessity to provide scattering information in the energetically closed channels. In the examples presented here, we overcome this difficulty by using simulated data. However, for future applications a practically feasible and problem orientated method for analytical continuation has still to be developed.

As already mentioned, the design of quantum devices via nanotechnology seems to be a potential field of application of these inverse scattering methods on the line (see also Ref.

[13]). In the presence of couplings between different electronic bands, the construction of profiles with specific reflection and/or transmission properties via fitting methods guided by intuition becomes rather difficult. Here, the developed coupled-channel inverse scattering methods can give a reliable guide line towards the required profile for the device. In this context the inclusion of bound states in the continuum in the inversion scattering procedure would be of great interest because slight changes in the retrieved profiles may result in sharp resonances which could be of interest for applications. Work is in progress to handle this important question from the inverse scattering point of view.

The presented formalism can be applied to any technological problem where one wants to retrieve or design the profile from the spectral information. Nanostructure devices and waveguides are obvious examples where these procedures can be of great interest.

### Acknowledgments

The authors gratefully acknowledge financial support from the the University of South Africa and the Vienna University of Technology.

## APPENDIX A: DERIVATION OF THE MARCHENKO EQUATION

The formulation of the solution of the ISP by means of an integral equation, frequently referred to as the Marchenko equation, is most easily achieved via the Levin representation of the Jost solution  $\mathcal{F}_-(k, x)$  (cf. Eq. (13)). In a first step we multiply Eq. (5) from the right by

$$\frac{1}{2\pi} \exp(-i\mathcal{K}y) \frac{d\mathcal{K}}{dk} \equiv \frac{1}{2\pi} \exp(-i\mathcal{K}y) \mathcal{K}^{-1} k, \quad (\text{A1})$$

substitute the Levin representations for  $\mathcal{F}_-(k, x)$  and  $\tilde{\mathcal{F}}_-(k, x)$  on the right hand side and integrate over  $k$ . Writing  $\mathcal{T}_L = \mathbf{1} + \Gamma(k)$  and reordering the terms leads to the relationship

$$\begin{aligned} \mathcal{I}_1 + \mathcal{I}_2 &= \tilde{\rho}_-(x, y) \\ &+ \int_{-\infty}^x dz \mathcal{B}_-(x, z) \tilde{\rho}_-(z, y) \int_{-\infty}^x dz \mathcal{B}_-(x, z) \mathcal{H}(z, y) \end{aligned} \quad (\text{A2})$$

with

$$\begin{aligned}
\mathcal{I}_1(x, y) &= \frac{1}{2\pi} \int_{-\infty}^{+\infty} dk k \mathcal{F}_+(k, x) \Gamma(k) e^{-i\mathcal{K}_y} \mathcal{K}^{-1} \\
\mathcal{I}_2(x, y) &= \frac{1}{2\pi} \int_{-\infty}^{+\infty} dk k [\mathcal{F}_+(k, x) - e^{-i\mathcal{K}_x}] e^{-i\mathcal{K}_y} \mathcal{K}^{-1} \\
\tilde{\rho}_-(x, y) &= \frac{1}{2\pi} \int_{-\infty}^{+\infty} dk k e^{-i\mathcal{K}_x} \mathcal{R}_L(k) e^{-i\mathcal{K}_y} \mathcal{K}^{-1} \\
\mathcal{H}(x, y) &= \frac{1}{2\pi} \int_{-\infty}^{+\infty} dk k e^{-i\mathcal{K}(x-y)} \mathcal{K}^{-1}.
\end{aligned}$$

In the presence of thresholds these integrals must be handled consistently and with care because of the  $(N - 1)$ -fold branch cut of the physical sheet of the Riemann surface for the momentum variable  $k$ . Because of the identity (A1) the  $j$ -th columns of the matrices  $\mathcal{I}_1$ ,  $\mathcal{I}_2$ ,  $\tilde{\rho}$ ,  $\mathcal{H}$  contain effectively integrals over the channel wave numbers  $k_j$ . It is therefore important to consider the consequences of the mapping of  $k$  to  $k_j$ , as given in Eq. (2). As displayed in Fig. 5 the integral over the real axis of  $k$  is transformed into a contour extending also to the positive imaginary axis of  $k_j$ ,  $j = 2, \dots, N$ .

To show the effect of this deformation of the contour we consider the matrix  $\mathcal{H}(x, y)$  which is diagonal with elements

$$\mathcal{H}_{jj}(x, y) = \frac{1}{2\pi} \int_{-\infty}^{+\infty} dk \frac{dk_j}{dk} e^{ik_j(x-y)} \quad (\text{A3})$$

with  $j = 1, \dots, N$ ,  $k_{11} \equiv k$ . Performing a transformation from  $k$  to  $k_j$  in the  $jj$ -element leads to a splitting of the integral

$$\begin{aligned}
H_{jj}(x, y) &= \frac{1}{2\pi} \int_{-\infty}^{+\infty} dk_j e^{ik_j(x-y)} \\
&\quad - i \frac{1}{2\pi} \int_{-\sqrt{\epsilon_j}}^{+\sqrt{\epsilon_j}} dk \frac{k}{\sqrt{\epsilon_j - k^2}} e^{-\sqrt{\epsilon_j - k^2}(x-y)}
\end{aligned} \quad (\text{A4})$$

Because of the symmetry of the integrand the second term of Eq. (A4) vanishes, while the first term yields the  $\delta$ -function. Hence we obtain  $\mathcal{H}(x, y) = \delta(x - y) \mathbf{1}$ .

Making use of the Levin representation of  $\mathcal{F}_-(x, y)$  we can apply the expression for  $\mathcal{H}(x, y)$  to evaluate  $\mathcal{I}_2(x, y)$ . Restricting ourselves to  $x > y$ , the matrix  $\mathcal{I}_2(x, y)$  vanishes and Eq. (A2) takes the simple form

$$\begin{aligned}
\mathcal{I}_1(x, y) &= \tilde{\rho}_-(x, y) + \mathcal{B}_-(x, y) \Theta(x - y) \\
&\quad + \int_{-\infty}^x dz \mathcal{B}_-(x, z) \tilde{\rho}_-(z, y)
\end{aligned} \quad (\text{A5})$$

where  $\Theta(x)$  is the Heavyside function.

In Eq. (A5) we are only left with the evaluation of the integral  $\mathcal{I}_1(x, y)$ . To evaluate  $\mathcal{I}_1(x, y)$  we close the integral in the upper-half plane of  $k$  in order to apply Cauchy's theorem. To do so we have to consider the integrand with regard to its analyticity. It is well known from scattering theory [3] that the occurrence of bound states leads to a pole of  $\mathcal{T}(k)$  and  $\mathcal{R}(k)$  on the positive imaginary axis of  $k$ . This is best seen from Eq. (5) where the requirement of a normalizable solution at  $k = q = i\kappa, \kappa > 0$  requires the relationship

$$\mathcal{F}_+(i\kappa, x) = \mathcal{F}_-(i\kappa, x) \lim_{k \rightarrow i\kappa} \mathcal{R}_L(k) \mathcal{T}_L^{-1}(k). \quad (\text{A6})$$

Employing a method similar to the one used in [6, 23], it can be shown that the poles of  $\mathcal{T}_L(k)$  at  $q_\alpha = i\kappa_\alpha$  are simple, i.e.

$$\mathcal{T}_L(k) = \frac{1}{k - q_\alpha} \mathcal{N}_\alpha + \dots, \quad (\text{A7})$$

where  $\mathcal{N}_\alpha$  is the residue of  $\mathcal{T}_L$  at  $k = q_\alpha$  and therefore also of  $\mathbf{\Gamma}_\alpha$ .

In the following we restrict ourselves to systems which have only true bound states at  $k^2 = q_\alpha^2 < 0, \alpha = 1, \dots, N_b$ . Thus the Jost solution is well defined in the upper half-plane of each channel wave number  $k_j$  and the integrand does not exhibit irregular features along the contour of integration. In order to evaluate the integral over the upper half circle we must consider the behavior of the  $\mathcal{F}(k, x)$  for  $|k| \rightarrow \infty$ . From Eq. (2) it immediately follows that

$$\text{Im } k_j = \text{Im } k \left[ 1 + \frac{1}{2} \frac{\epsilon_j}{|k|^2} + o\left(\frac{\epsilon_j^2}{|k|^4}\right) \right].$$

Hence, the dominant term for the vanishing of the Jost solution in the upper half plane of  $k$  for  $|k| \rightarrow \infty$  is independent of the channel and leads to a vanishing of the integral over the half circle for  $x > y$ . Thus the integral  $\mathcal{I}_1(x, y)$  is simply given by the sum over all bound state poles

$$\mathcal{I}_1 = i \sum_{\alpha=1}^{N_b} \mathcal{F}_+(q_\alpha, x) \mathcal{N}_\alpha \exp(-i\mathcal{Q}_\alpha y) \mathcal{Q}(q_\alpha)^{-1} q_\alpha, \quad (\text{A8})$$

where we assume that the potential  $\mathcal{V}(x)$  sustains  $N_b$  bound states.

Using the specific relationship, Eq. (A6), between the Jost functions  $\mathcal{F}_+$  and  $\mathcal{F}_-$  at the bound states,  $k = q_\alpha$ , and entering the Levin representation for  $\mathcal{F}_-(k, x)$  leads finally to

$$\mathcal{I}_1(x, y) = -\tilde{\rho}_-^{(b)}(x, y) - \int_{-\infty}^x dz \mathcal{B}_-(x, z) \tilde{\rho}_-^{(b)}(z, y) \quad (\text{A9})$$

with

$$\tilde{\rho}_{-}^{(b)}(x, y) = - \sum_{\alpha=1}^{N_b} \exp(-i\mathcal{Q}_{\alpha}x) i\mathcal{M}_{\alpha} \exp(-i\mathcal{Q}_{\alpha}y) \mathcal{Q}_{\alpha}^{-1} q_{\alpha} \quad (\text{A10})$$

where  $\mathcal{M}_{\alpha}$  are the residues of  $\mathcal{R}_L(k)$  at  $q_{\alpha}$ . Introducing the total input kernel

$$\rho_{-}(x, y) = \tilde{\rho}_{-}(x, y) + \tilde{\rho}_{-}^{(b)}(x, y) \quad (\text{A11})$$

leads to the Marchenko equation (20).

## APPENDIX B: DEFINITION OF POTENTIAL PROFILES

In the examples we use potentials, whose elements are given by an  $x$ -dependence of closed form. In the following we summarize the definitions of the potential forms and their parameters.

### 1. Gaussian Profile

$$V(x) = V_0 \exp(-b(x - c)^2) \quad (\text{B1})$$

### 2. Multilayer Profile

$$V(x) = \sum_{i=1}^N V_i \left[ \frac{1}{1 + \exp((x_{i-1} - x)/a)} - \frac{1}{1 + \exp((x_i - x)/a)} \right], \quad (\text{B2})$$

where  $N$  is the number of layers,  $a$  is the diffuseness parameter, and  $V_i$  the strength of the layer with width  $x_i - x_{i-1}$  with  $x_0$  being the left boundary of the multilayer profile.



### 3. Multiple Sea-Saw Potential

The sea-saw potential is defined by

$$V(x) = \frac{2 V_0}{x_\ell} \begin{cases} 0 & x < x_0 \\ s_m (x - x_{m-1}) & x_{m-1} \leq x \leq \bar{x}_m \\ s_m (x_m - x) & \bar{x}_m \leq x \leq x_m \\ 0 & x_{n_s} < x \end{cases}, \quad m = 1, \dots, n_s \quad (B3)$$

where  $x_m = x_s + mx_\ell$  and  $\bar{x}_m = x_s + (m - \frac{1}{2})x_\ell$ ,  $m = 1, \dots, n_s$ . Here,  $n_s$  is the number of sea-saw peaks of length  $x_\ell$ ,  $V_0$  is the strength of the potential, and  $s_m$  is the sign of the corresponding term. The nonvanishing part of the profile is shifted by an amount  $x_s$  from the origin. Thus it extends between  $x_0$  and  $x_{n_s}$ .

- 
- [1] I. Kay, *Comm. Pure Appl. Math* **13**, 371 (1960).
  - [2] Z. S. Agranovich and V. A. Marchenko, *The Inverse Problem of Scattering Theory*, (Gordon & Breach, New York, 1963).
  - [3] K. Chadan and P. C. Sabatier, *Inverse Problems in Quantum Scattering Theory*, 2nd ed. (Springer, New York, 1989).
  - [4] G. L. Lamb, *Elements of Soliton Theory* (Wiley, New York), 1981.
  - [5] D. N. Ghosh Roy, *Methods of Inverse Problems in Physics* (CRC Press, Boston, 1991).
  - [6] M. Wadati and T. Kamijo T, *Prog. Theoret. Phys.* **52**, 397 (1974).
  - [7] F. Calogero and D. Degasperis, *Nuovo Cimento* **32B**, 201 (1976); **39B**, 1 (1977).
  - [8] S. A. Sofianos, M. Braun, R. Lipperheide, and H. Leeb, *Lecture Notes in Phys.* **488**, 54 (1997).
  - [9] J. M. Cowley, *Diffraction Physics* (North Holland, Amsterdam), 1975.
  - [10] R. E. Burge, M. A. Fiddy, A. H. Greenaway, and G. Ross, *Proc. Roy. Soc. London* **A 350**, 191 (1976).
  - [11] M. V. Klivanov and P. E. Sacks, *J. Math. Phys.* **33**, 3813 (1992).
  - [12] J. Kasper, H. Leeb and R. Lipperheide, *J. Magn. Magn. Mat.* **196**, 51 (1999).

- [13] Microelectronics Journal **30** (1999). The whole volume is devoted to various aspects of semiconductor quantum devices.
- [14] M. Braun, S. A. Sofianos, and R. Lipperheide, Inverse Problems **11**, L1 (1995).
- [15] E. Witten, Nucl. Phys. B **188**, 51 (1981).
- [16] D. Baye, Phys. Rev. Lett. **58**, 2738 (1987); Phys. Rev. A **48**, 2040 (1993).
- [17] C. V. Sukumar, J. Phys. A: Maths. Gen. **18**, L57 (1985); **18**, 2917 (1985); **18**, 2937 (1985).
- [18] L. Infeld and T. E. Hull, Rev. Mod. Phys. **23**, 21 (1951).
- [19] R. D. Amado, F. Cannata, J.-P. Dedonder, Phys. Rev. Lett. **61**, 2901 (1987); Int. J. Mod. Phys. A **5**, 3401 (1990).
- [20] J.-M. Sparenberg and D. Baye, Phys. Rev. Lett. **97**, 3802 (1997).
- [21] R. G. Newton, *Scattering Theory of Waves and Particles*, 2nd ed. (Springer, New York, 1982).
- [22] H. Leeb, S. A. Sofianos, J.-M. Sparenberg, and D. Baye, Phys. Rev. **C 62**, 064003 (2000).
- [23] H. A. Weidenmüller, Ann. Phys. (N.Y.) **29**, 60 (1964).

## FIGURE CAPTIONS

### Figure 1

Reconstructed potential (dashed line) of a 2-channel system without thresholds or bound states. The details of the original potential (solid line) are given in the text.

### Figure 2

Reconstructed potential (solid line) of a coupled 2-channel system with a threshold  $\epsilon_2 = 0.025$  in the 22-channel. The details of the original potential (dashed line) are given in the text.

### Figure 3

Reconstructed potential (dashed line) of a two-channel system with a bound state but without thresholds. The original potential (solid line) is shown for comparison.

### Figure 4

Input potentials (solid line) and the SUSY transformation potentials (dashed line).

### Figure 5

Mapping of  $k$  to  $k_j$  and the corresponding deformation of the contour for integration.

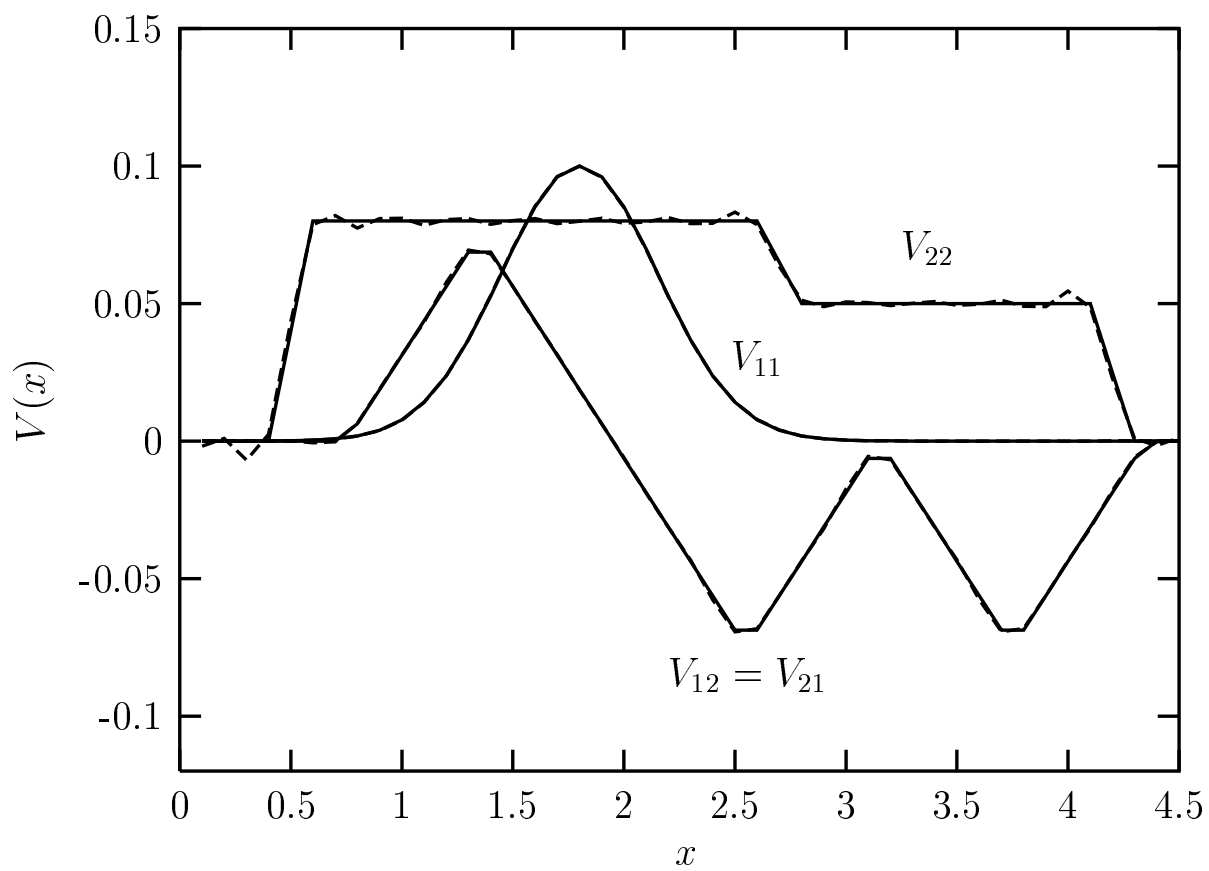
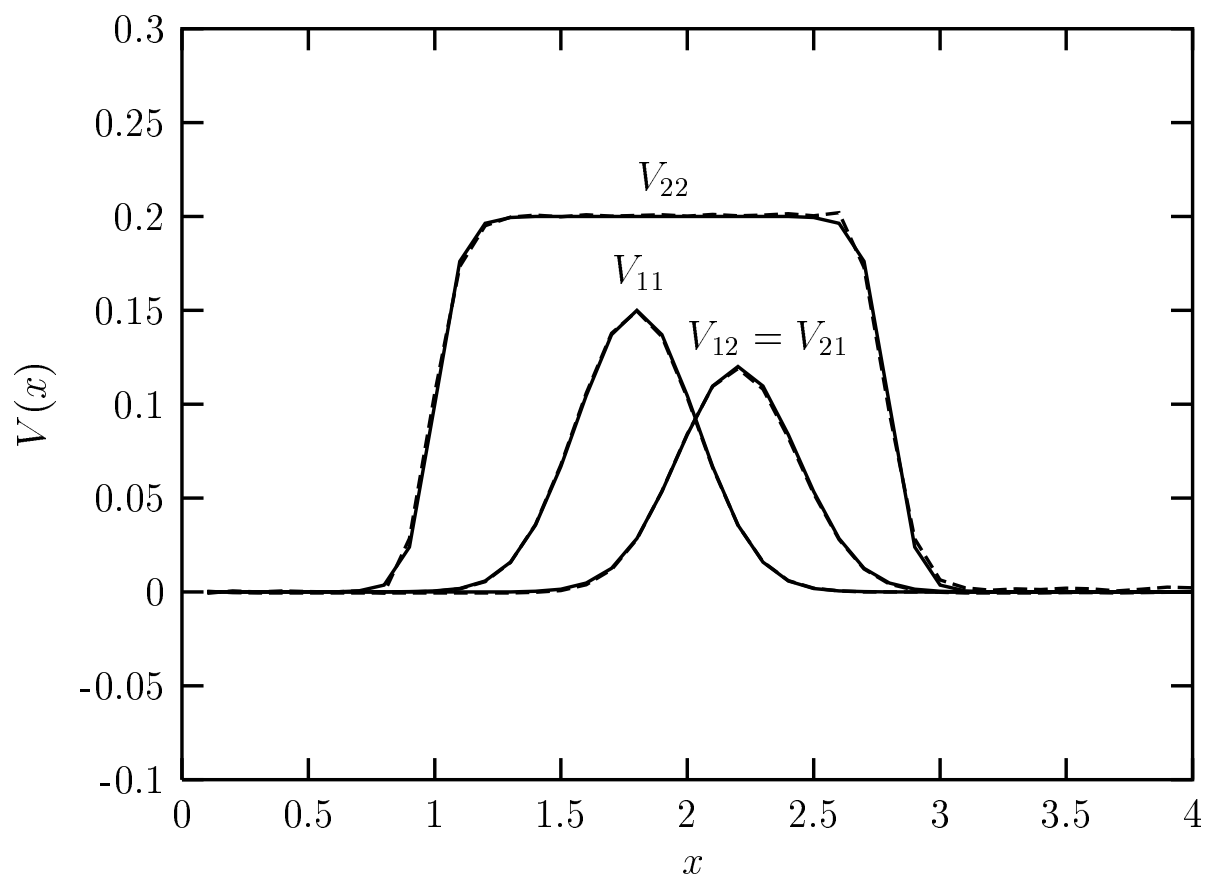
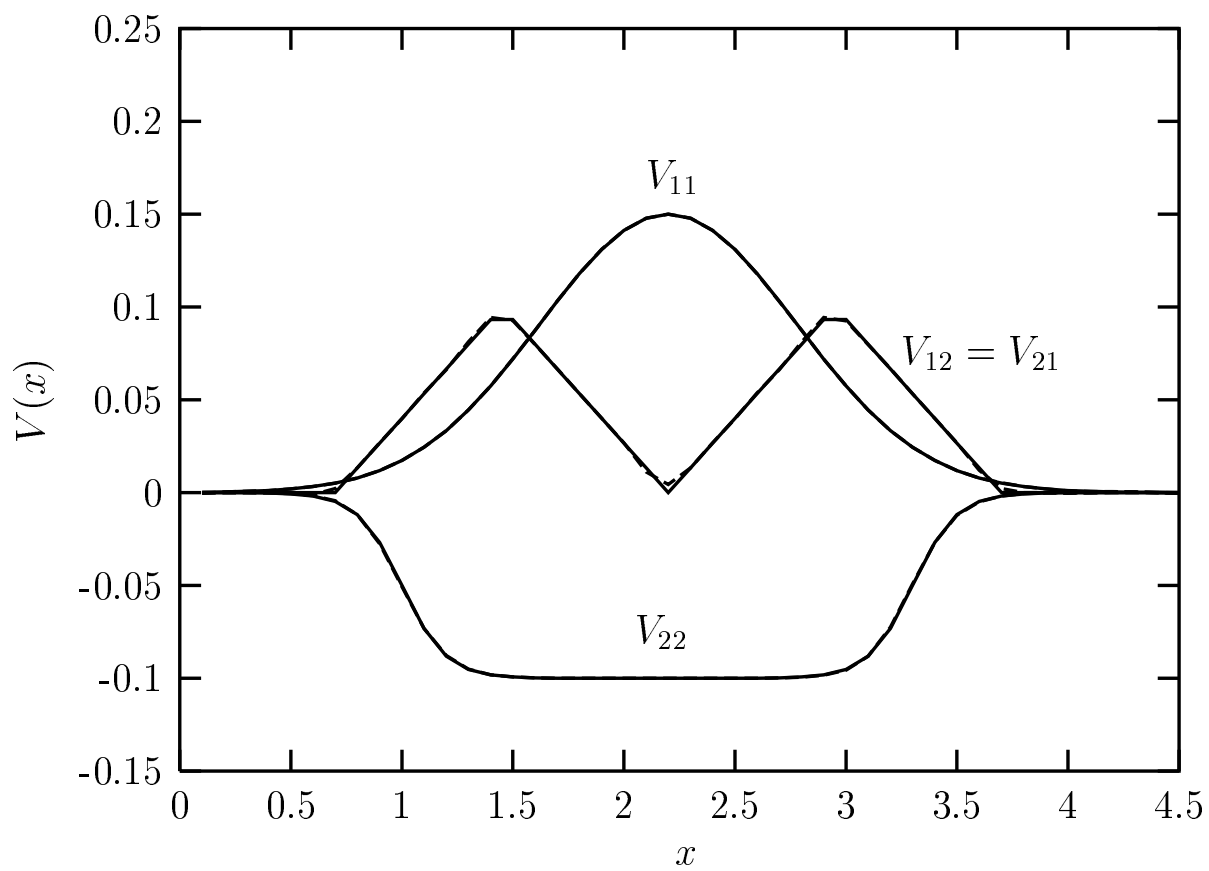


Figure 1



**Figure 2**



**Figure 3**

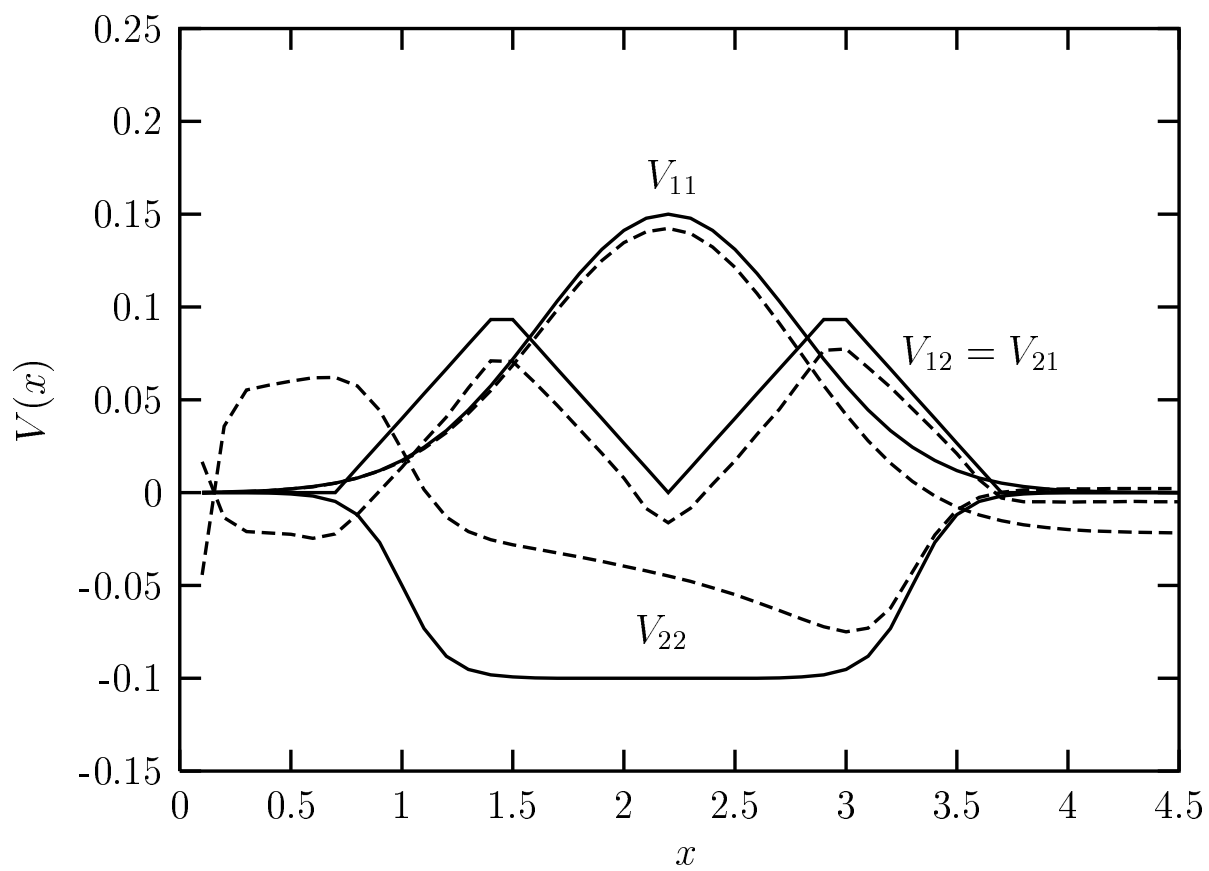


Figure 4

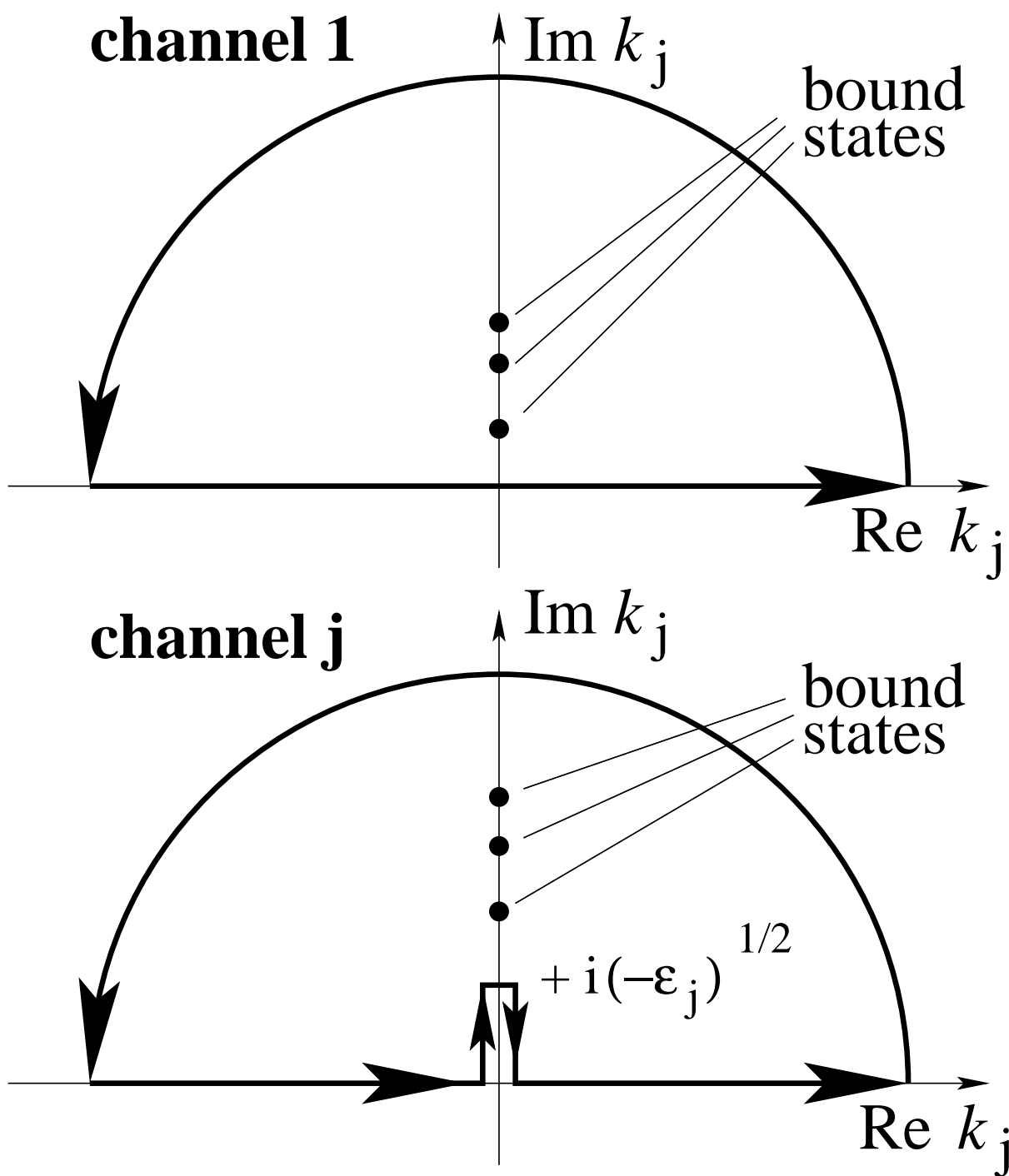


Figure 5